Morphological examination of the NP-28 submarine channel-fan complex in the Amundsen Basin, Arctic Ocean

Kai Boggild

Submitted in Partial Fulfilment of the Requirements
For the Degree of Bachelor of Sciences, Honours
Department of Earth Sciences
Dalhousie University, Halifax, Nova Scotia
March 2016

Distribution License

DalSpace requires agreement to this non-exclusive distribution license before your item can appear on DalSpace.

NON-EXCLUSIVE DISTRIBUTION LICENSE

You (the author(s) or copyright owner) grant to Dalhousie University the non-exclusive right to reproduce and distribute your submission worldwide in any medium.

You agree that Dalhousie University may, without changing the content, reformat the submission for the purpose of preservation.

You also agree that Dalhousie University may keep more than one copy of this submission for purposes of security, back-up and preservation.

You agree that the submission is your original work, and that you have the right to grant the rights contained in this license. You also agree that your submission does not, to the best of your knowledge, infringe upon anyone's copyright.

If the submission contains material for which you do not hold copyright, you agree that you have obtained the unrestricted permission of the copyright owner to grant Dalhousie University the rights required by this license, and that such third-party owned material is clearly identified and acknowledged within the text or content of the submission.

If the submission is based upon work that has been sponsored or supported by an agency or organization other than Dalhousie University, you assert that you have fulfilled any right of review or other obligations required by such contract or agreement.

Dalhousie University will clearly identify your name(s) as the author(s) or owner(s) of the submission, and will not make any alteration to the content of the files that you have submitted.

If you have questions regarding this license please contact the repository manager at dalspace@dal.ca.

Grant the distribution license by signing and dating below.

_____ _____

Name of signatory Date

Abstract

Submarine channels are common features along continental margins, yet relatively little is known about how these systems behave at polar latitudes. Emerging hypotheses concerning the influence of Coriolis effect on these systems predict that straighter geometries will dominate at high latitudes due to the increased Coriolis forcing of sediment-laden currents. This research examines the morphology of the NP-28 submarine channel in the Amundsen Basin and evaluates its form in the context of inertial and Coriolis forcing. At latitudes between 85° and 90° N, the NP-28 submarine channel is the northernmost modern submarine channel on Earth and offers a promising opportunity to test models of high latitude submarine channels. This study uses recently acquired multibeam bathymetry to provide the first plan-view constraints on channel path and high resolution subbottom profiler data to describe turbidite system elements at a finer vertical resolution than previously possible.

The NP-28 submarine channel is an example of a low-gradient, low-sinuosity channel, broadly fitting recently identified global trends in peak channel sinuosity relative to latitude. The modern geometry of the channel is likely to have been established by a combination of suspension and traction-dominated flow regimes resulting in the formation of external and confined levees. Subbottom profiler data further reveal the nature of these deposits, as well as other elements of the channel system including low-amplitude sediment waves, external levee sediments and a distributary channel on the lower fan surface.

Consistent right-dominant levee asymmetries of external levee deposits indicate that Coriolis forces dominate for suspension-dominated regimes. Rossby numbers calculated based on morphometrically estimated bankfull flow velocities are consistently low. The geometry of intrachannel deposits and thalweg incision, however, appears to be consistent with experimental models for both high latitude and equatorial channels, indicating that the relative influence of Coriolis forces to centrifugal forces may vary along the channel length for faster, traction-dominated flows in the NP-28 channel.

Keywords: Submarine channels; turbidity currents; Coriolis effect; Amundsen Basin; sinuosity;

Acknowledgements

Firstly, I would like to thank my supervisor, Dr. David Mosher for fantastic mentorship guidance through this thesis and in past projects. This project has been incredibly fascinating to research, and to consider the linkages between a spinning Earth and surface processes has been a great experience.

This project would not have been possible without support from the Geological Survey of Canada and the Canadian Hydrographic Service. I would very much like to thank everyone involved in the collection of the data used in this project, including the crew and scientific personnel aboard *CCGS Louis S. St-Laurent*. I would also like to thank Paola Travaglini and Walli Rainey for helping me prepare the data used in this project, as well as anyone else who I have brainstormed ideas with in the past year. I would also like to thank honours coordinator Lawrence Plug for running the honours seminars and providing me with some great edits.

A big thank you goes to my parents, family and friends for their support during this project. Finally, I would also like to thank all the people, instructors, and students at Dalhousie for making for a wonderful undergraduate experience.

Table of Contents **Page**

List of Figures **Page**

List of Tables **Page**

List of Equations **Page**

1.0 Introduction

1.1 Opening Statement

Submarine channels are common features along continental margins and are one of the most volumetrically important pathways for sediment delivery to the deep sea (Wynn et al., 2007). Because of this, these systems are of considerable importance to the understanding of the global carbon cycle, sediment budgets and paleoclimate (Wynn et al., 2007). These channels are built by the action of downslope turbidity currents and may stretch up to thousands of kilometers across the seafloor. They typically are the conduits for sediment supply to deep water fans; some of which are the largest depo-centres in the World.

Modern submarine channel systems exhibit a wide range of geometries from highly sinuous (e.g. Amazon, Indus) to poorly sinuous or straight channel systems (e.g. Bounty Channel, Northwest Atlantic Mid Ocean Channel). The sinuosity of these submarine channel systems has long been understood to be influenced by slope, sediment type and sediment flux (Clark et al., 1992). Recent observations, however, have also documented an apparent global relationship between peak channel sinuosity and latitude, in which high latitude systems maintain straighter channel paths than their equatorial counterparts (Peakall et al., 2012). Emerging hypotheses suggest that these changes may due, in part, to increased strength of Coriolis forces at high latitudes (Peakall et al., 2012) which may provide mechanisms for maintenance of straighter channel geometries (Cossu et al., 2015).

Until recently, little empirical data of submarine channels at polar latitudes existed due to the challenges inherent in collecting geophysical and bathymetric data in perennially ice-covered seas. Data were collected in these regions in recent years, however, due in part to Arctic coastal State's extended continental shelf mapping initiatives. These new data have led to improved resolution and discovery of new submarine channel systems (e.g. Mayer et al., *In press*).

The NP-28 channel-levee complex was first identified in 2004 by Kristoffersen et al., using a limited dataset, and is the northernmost submarine channel on Earth. The NP-28 channel flows from the Klenova Valley into the Amundsen Basin in the greater Arctic Ocean at latitudes between 85° and 90° N. Among other interpretations, this channel was predicted to be highly sinuous due to its low bathymetric gradient (Kristoffersen et al., 2004) citing well-established

relationships between channel slope and sinuosity (Clark et al 1992). Since the original description of the channel, new datasets were collected in the Amundsen Basin, including multibeam bathymetry data which provide the first plan-view constraints on channel morphology. These data offer a unique opportunity to observe a potential end-member in recently described relationships between channel geometry and latitude.

1.2 Thesis Objective

The objective of this thesis is to examine the morphology and evolution of the NP-28 submarine channel, and in doing so, assess the influence of Coriolis on high latitude deep sea submarine channels. In this study, multibeam data are used to provide the first plan-view description of the channel morphology. These data are coupled with CHIRP 3.5 kHz subbottom profiler data to provide information in the third dimension and examine turbidite system elements. It is hypothesised that Coriolis forces at these latitudes play a significant role in the development of channel/levee complexes, and that the NP-28 channel is an example of a low-gradient, low-sinuosity channel. This study will also use morphometric approaches of estimating bankfull flow velocities to better constrain the importance of Coriolis force relative to inertial force (Rossby number).

2.0 Background

2.1 Geologic Setting

The Amundsen Basin (Figure 2.1) is the northern sub-basin of the Eurasian Basin which was formed by seafloor spreading along Gakkel Ridge, initiating at approximately 57 Ma (Moore et al. 2006, Jokat et al. 1992). Spreading along Gakkel Ridge coincided with rifting of Lomonosov Ridge, an 1800 km-long blocky continental fragment, from the Barents-Kara Sea margin (Moore et al. 2006). Seismic refraction studies and results from the International Ocean Drilling Program ACEX site confirm that this structure was once stratigraphically consistent with the Barents-Kara Sea and Ellesmere margins (Moore et al., 2006, Jackson et al. 2010). Once seafloor spreading was initiated, sediment thickness asymmetries between the Amundsen and Nansen Basins indicate that the Amundsen Basin received less sediment than the Nansen Basin, likely as a result of being geographically isolated from shelf sediments coming from the Barents Sea margin (Jokat and Micksch 2004).

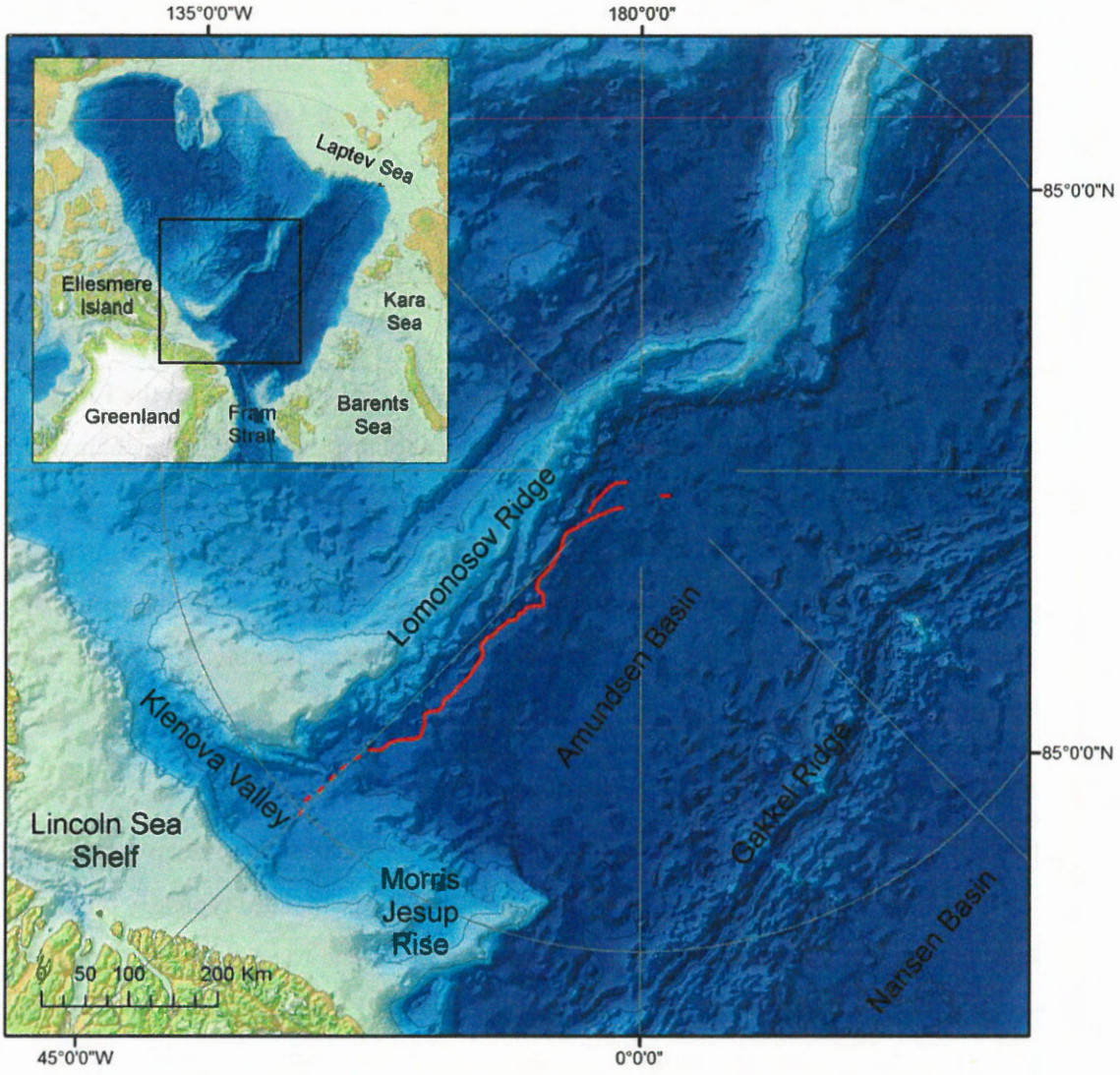

Figure 2.1 International Bathymetric Chart of the Arctic Ocean (IBCAO) V3.0 basemap of the Amundsen Basin and surrounding areas. The location of the NP-28 channel is shown in red.

Stratigraphic information about Amundsen Basin fill consists primarily of seismic data, however there exists a small number of gravity, trigger and piston cores distributed throughout the basin which yield information on the near-surface stratigraphy (Backman et al., 2004). Most estimates of Quaternary sedimentation rates from sediment cores in the Eurasian Basin suggest rates on the order of one cm ka^{-1} (Backman et al., 2004).

A bathymetric saddle known as the Klenova Valley lies between the southern margin of Lomonosov Ridge and the Lincoln Sea margin (GEBCO 2003). The valley opens into the

Lincoln Sea and deepens towards the Amundsen Basin between Lomonosov Ridge and Morris Jessup Rise. Recent gravity inversion models suggest a 7km deep sedimentary basin/basement depression underlies Klenova Valley, likely part of the 600 km long Lomonosov-Klenova Fault Zone interpreted to be the result of crustal shortening during the Eurekan Orogeny (Døssing et al, 2014). Outlines of a 200 km by 400 km depocenter in the Amundsen Basin from these gravity inversion models further predict that substantial sediment transfer into the basin has occurred via the Klenova Valley (Døssing et al 2014),

The NP-28 submarine channel extends through the Klenova Valley from the Lincoln Sea and into Amundsen Basin, between latitudes of approximately 85° to 90° N. The channel was originally described by Kristoffersen et al. (2004) as an aggradational channel with a consistent right-dominant levee asymmetry. They suggest it was the result of turbidity currents, influenced by the Coriolis effect, flowing from a bathymetric saddle between Lomonosov Ridge and the Lincoln Sea margin, supplying sediment to a deep sea fan extending into the Amundsen Basin and beyond the North Pole.

2.2 Submarine Channels

Submarine channels are major conduits for sediment delivered to the deep ocean. They commonly develop as sediment tributaries to large submarine fans and are typically the result of sediment laden turbidity currents which erode and deposit sediment to produce characteristic channel-levee complexes along continental margins (Clark and Pickering 1996). Most modern (active) submarine channels are associated with deep sea fans seaward of large river systems with high sediment input (e.g., Indus Fan, Nile Fan, Amazon Fan). Many more deep sea channels are apparent on the present-day seafloor, but are apparently inactive. These systems developed during sea-level lowstand conditions in which riverine or glacial outwash sediment flux reached the shelf break and fed directly to deep water (Wynn et al., 2007). These have become dormant or near dormant during Holocene high sea level conditions (Clark et al. 1992, Wynn et al 2007).

2.2.1 Channel Planform Morphology

Slope gradient, sediment flux rates and grain size are known to influence the planform morphologies of submarine channels (Clark et al., 1992). This fact was demonstrated by Clark et al. (1992), who documented key morphological parameters including slope, meander radius,

wavelength and sinuosity. In this work, data from 16 different channel systems were used to illustrate that submarine channel systems appear to reach a maximum sinuosity at their approximate middle slope position (Figure 2.2).

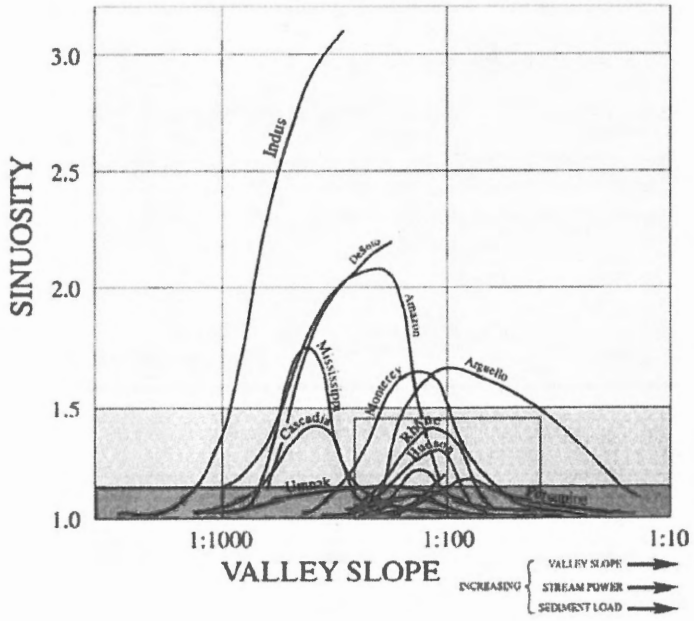

Figure 2.2 Sinuosity curves of major submarine channel systems with changing valley slope (from Clark et al., 1992).

Clark et al., (1992) also suggested that differences in slope between these channel systems may be important in determining peak sinuosities. They observed that steeper channel systems tended toward higher sinuosities, and channels built by flows with a coarser bedload tended to be straighter than systems with finer sediment load (Clark et al. 1992). These observations provided the basis for a channel classification scheme based on slope and planform morphology in which there are two end members; low-gradient high-sinuosity channels and high-gradient low-sinuosity channels (Clark et al. 1992). Later, Klaucke et al., (1997) described the North Atlantic Mid Ocean Channel (NAMOC) as a low-sinuosity/low gradient channel, suggesting that the binary classification scheme of Clark et al. (1992) may not be inclusive of all submarine channels.

Channel sinuosity of an equilibrium channel is developed by the amplification of meanders along a channel path (Figure 2.3). Initiation of submarine channel sinuosity is still poorly understood, and elusive to model (Wynn et al., 2007). It is thought that these meanders

are initiated by perturbations in the initial flow path, which deflect the flow causing erosion along the outer bank and deposition along an inner bank (Cossu et al., 2015). Progressive amplification of channel meanders results in the accretion of point-bar like intra-channel deposits downstream of the inner bank and erosion on the outer bank (Peakall et al., 2007).

Unlike fluvial channel systems, the amplification of meanders in submarine channel systems does not necessarily coincide with substantial downstream translation of the meander bend (Figure 2.3) (Peakall et al., 2000). Instead, meanders amplify nearly perpendicular to the channel axis and may even approach a stable equilibrium planform geometry (Peakall et al., 2000).

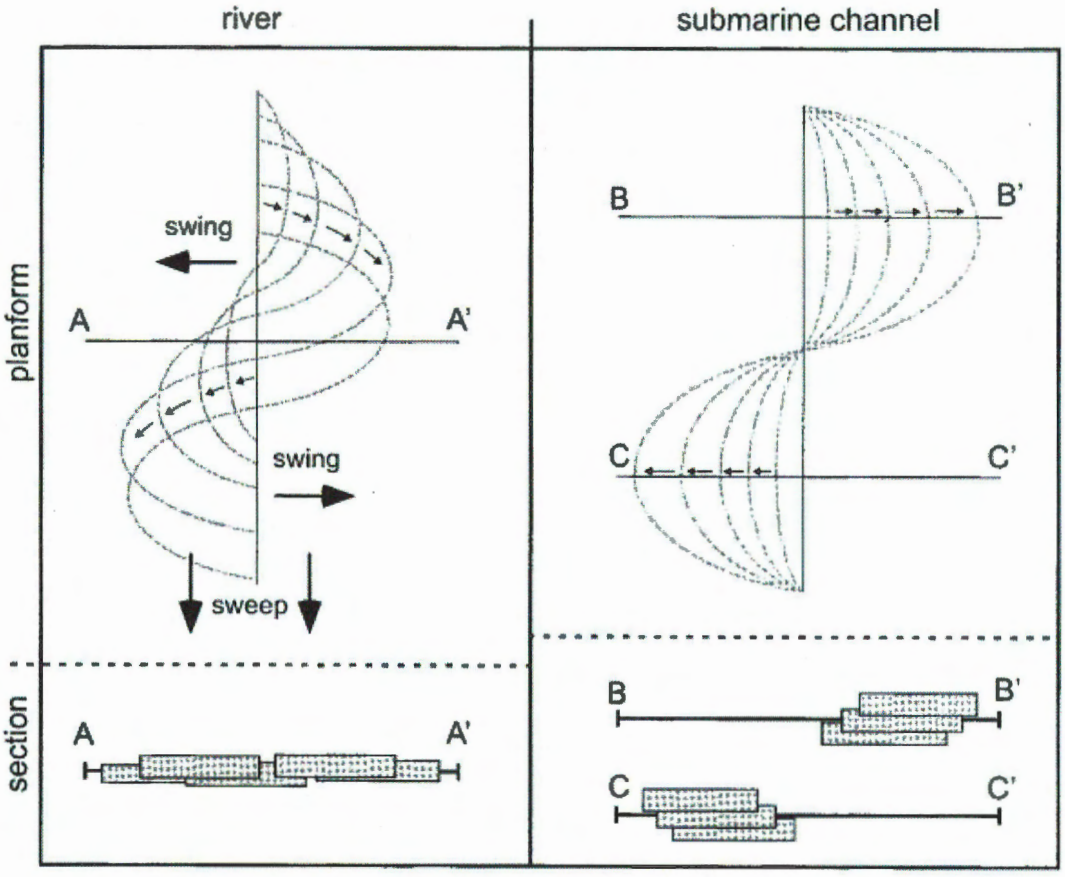

Figure 2.3 Comparison between sinuosity development styles of fluvial and submarine channels. Stippled bars represent geometries of channel bodies deposited in an aggrading channel (from Peakall et al., 2000).

2.2.2 Channel Longitudinal Morphology

Examination of a global dataset of longitudinal profiles of canyon-channel complexes by Covault et al., (2011) resulted in three major morphological groupings: convex, slightly concave and very concave (Figure 2.4). These are interpreted to be representative of different marginal settings from which these systems originate (Covault et al., 2011). Convex profiles are broadly observed along margins with substantial tectonic uplift and synsedimentary deformation (Covault et al., 2011). Very convex profiles generally coincide with channels along young, underdeveloped margins in which steep slopes and narrow shelves promote erosion by sediment or gravity flows (Covault et al., 2011).

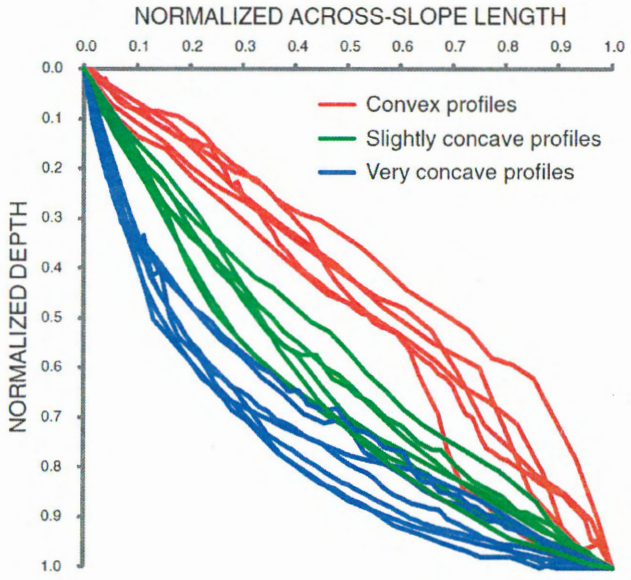

Figure 2.4 Morphological groupings of longitudinal profiles showing convex, slightly concave and very concave profiles (from Covault et al., 2011).

With a few exceptions, it was found that channels located along mature passive margins follow slightly concave longitudinal profiles (Covault et al., 2011). These profile styles are observed for mature fan systems such as the Amazon Fan channel (e.g. Pirmez and Flood 1995), where uplift/deformation is negligible (Covault et al., 2011). In these settings, modern channels are substantially influenced by the pre-existing depositional architecture of fan deposits which promote longitudinal profiles that are less concave than immature margins (Covault et al., 2011). These slightly concave profiles are considered the equilibrium condition for submarine channel

systems, and are analogous to logarithmic equilibrium profiles of riverine channels (Pirmez et al., 2000).

The equilibrium profile of submarine channels may be disrupted by tectonic deformation, changes in sediment flux, or changes in base level caused by channel avulsion (Pirmez et al., 2000). Where disrupted, these profiles may exhibit knickpoints, where gradient is locally increased (Pirmez et al., 2000). Re-establishment of the equilibrium profile is thought to occur by rapid headward erosion and infill at the base (Pirmez et al., 2000). In channels where this process is incomplete, subdued knickpoints can be observed in longitudinal profiles of modern channels (Figure 2.5).

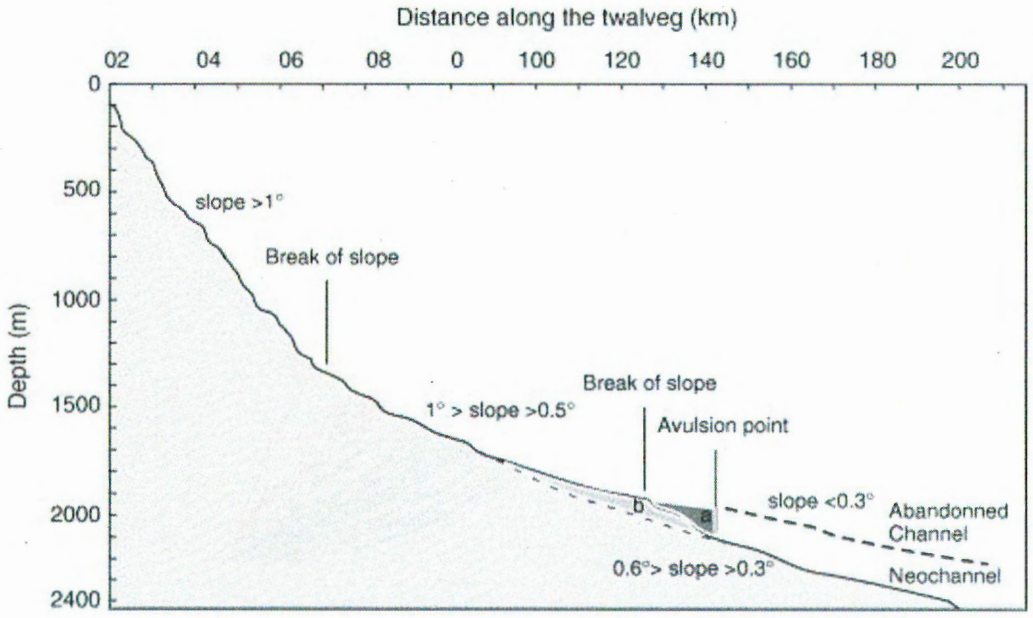

Figure 2.5 Longitudinal profile of the Rhône Channel showing a subdued knickpoint (break in slope) upstream of a channel avulsion point (from Bonnel et al., 2005)

2.3 Architectural Elements of Submarine Channel/Fan Complexes

To enable comparisons between channel/fan systems, sequences and morphologies of these systems may be described in terms of architectural elements (Mutti and Normark, 1991). There have been several attempts to categorize architectural elements for deep sea channel/fan systems (e.g. Mutti and Normark 1991, Piper and Normark 2001). This study will adopt the hierarchy of Mutti and Normark (1991) who propose a set of five primary architectural elements

to describe these systems that include; channels, overbank deposits, erosional features, lobes and channel-lobe transition deposits. These elements are defined as mappable features which are likely to occur in a broad range of turbidite systems and are the result of genetically comparable processes.

Channel Element

The channel element, as previously discussed, is further subdivided into two groups; large leveed channels and small un-leveed channels (Mutti and Normark 1991). Large channels that are bounded by large aggraded levee deposits typically act as main sediment pathways through which large amounts of suspended sediment are transported or bypassed towards the abyssal fan lobes (Mutti and Normark, 1991). Smaller, un-leveed channels are typical of distributary channels and occur on scales that are one or two orders of magnitude smaller than large channels (Mutti and Normark 1991).

Channels are also classified based on their erosional or depositional characteristics, which recognizable in cross-section or seismic profile (Figure 2.6). Depositional or aggradational channels are characterized by raised channel floors and prominent levees with continuous reflections (Clark and Pickering 1996). Erosional channels are characterized by truncated reflections, and may exhibit down-cutting structures such as terraces formed by an erosive current (Clark and Pickering 1996). Depositional-erosional channels generally have characteristics of both depositional and erosional styles.

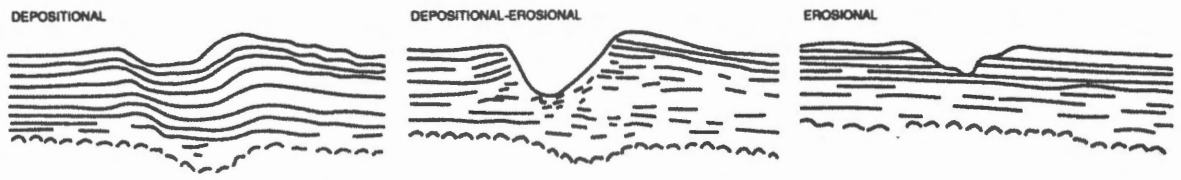

Figure 2.6 Schematic of modern depositional, depositional-erosional and erosional channel styles (from Clark and Pickering 1996).

Other Elements

The overbank deposit element consists of laterally extensive sediments deposited by overbanking flows from a related channel (Mutti and Normark, 1991). These sediments are typical of aggraded levees that bound channels, and may be deposited by channel systems with

varying amounts of relief (Mutti and Normark, 1991). These sediments thin with perpendicular distance to the channel axis, and may exhibit sediment waves trending parallel or oblique to the channel

Depositional lobes are morphologically distinguished in modern fan systems by their lobate form and occur downslope of the termination of a large channel system (Mutti and Normark, 1991). These lobes are characterized by the deposition of sand-rich sediments that may appear acoustically transparent and have small un-leveed channel systems on their surface (Mutti and Normark 1991).

The understanding of the channel-lobe transition deposit element is the least constrained by observations of modern fans due to the fine spatial scale of distinguishing characteristics (Mutti and Normark, 1991). This element represents the transition between channelized turbidite deposition and lobe deposition at the channel terminus, and thus is represented by both erosional and depositional features that are observed in channel and lobe elements (Mutti and Normark, 1991). These transition zone deposits are usually characterized by localized erosion or breaks in slope.

Erosional elements include a variety of large scale features common to channel/fan systems, including; canyons, shelf-edge indentations, slope failures and failures within basin turbidites (Mutti and Normark, 1991). Due to the broad nature of this element, it may be used to describe several components of channel/levee systems; however, its main importance is considered to be the potential for source sediment derived from these erosional features for downslope turbidite deposition (Mutti and Normark, 1991).

The development of different elements in turbidite channel systems is influenced by different flow types. Normark and Piper (1991) consider the influence of these variations in flow types on the architecture of these systems. Generally, flow types with substantial suspended sediment such as large muddy flows or repeated thin muddy flows will contribute to the development of external levee deposits, whereas large sandy flows will contribute to deposition of sand in the channel axis and on depositional lobes at the termination of the channel.

2.4 Coriolis Forces

Since the Earth is a naturally rotating reference frame, an object or flow moving along a straight trajectory through a fluid on the Earth's surface (e.g. the ocean) will appear to experience a deflected path. This apparent deflection is known as the Coriolis effect, and is related to the fact that the linear velocity of the Earth's rotation is maximum at the equator and minimum at the poles (i.e. a fixed point on the Earth's surface will travel faster at the equator than a fixed point near the pole). The flow will appear to deflect across the surface of the Earth as it moves since it's linear and angular momentum are conserved. Deflection by the Coriolis effect is only apparent in the rotating reference frame (e.g. the Earth); in fact, there is no deflection in the non-rotating inertial reference frame.

The magnitude of the apparent deflection is a function of the rotation rate of the Earth (angular velocity) (Ω) and latitude (θ) as described by the Coriolis parameter (f) (Equation 2.4.1).

$$f = 2\Omega\sin\theta \qquad (2.4.1)$$

The absolute value of the Coriolis parameter increases with distance from the equator, reaching a maximum at the poles where the sine of latitude approaches 1; the angular velocity is assumed constant. In the northern hemisphere, the Coriolis parameter is considered positive and there is an apparent deflection to the right, whereas in the southern hemisphere, a negative Coriolis parameter is associated with deflection to the left. The Coriolis parameter influences the strength of Coriolis forces which cause the deflection relative to the rotating reference frame. Coriolis force is an inertial force (i.e. fictitious force), and is the result of the rotating reference frame only.

Coriolis forces were first thought to influence the development of submarine channels when bathymetry of submarine fans in the northeast Pacific showed that related channels often exhibited a leftward hook (Menard 1955). While notably opposite to the expected Coriolis deflection in the northern hemisphere, it was suggested that this leftward hook may be a result of Coriolis forces causing preferential building of the right-hand levee, forcing the channels to turn to the left (Menard 1955). Since then, similar observations of levee height asymmetries in other channel systems show that northern hemisphere channel-levee systems tend towards a taller

right-hand levee, whereas southern hemisphere systems characteristically show the opposite levee asymmetry (Figure 2.7).

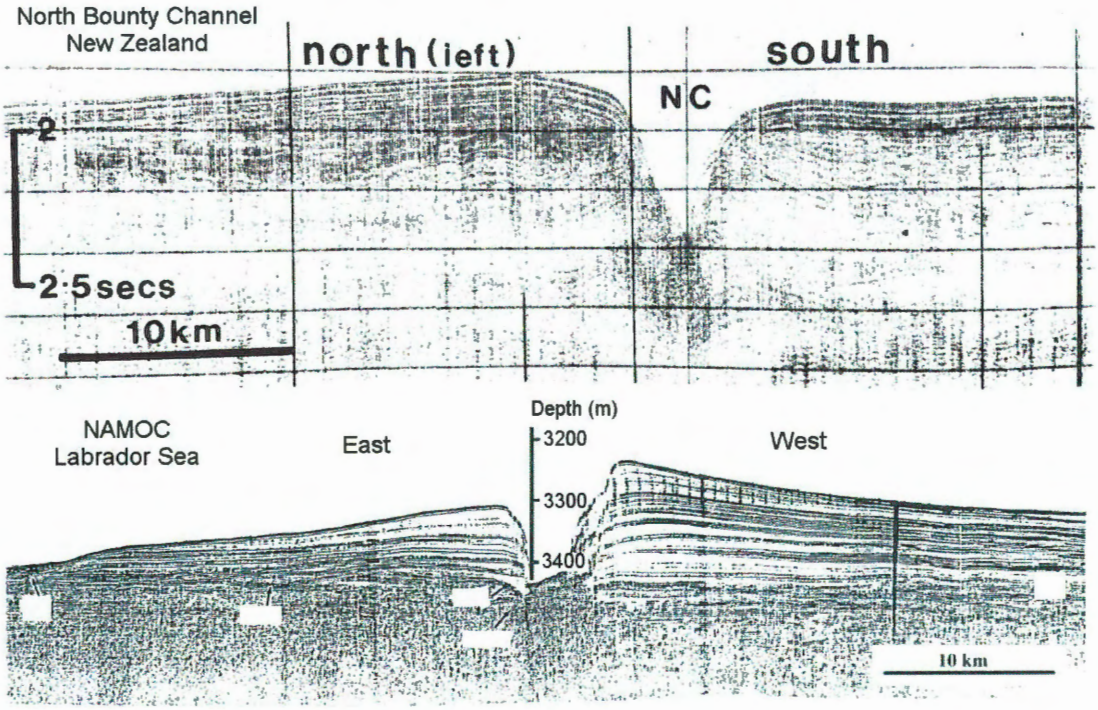

Figure 2.7 Top: Single channel seismic profile of the northern branch of a channel-levee system at ~46°S in the Bounty Trough, New Zealand showing left-hand dominant levee asymetry (from Carter and Carter, 1988). Bottom: Seismic profile of NAMOC in the Labrador Sea ~59°N (modified from Klaucke et al., 1998). Both sections are oriented looking down-channel.

2.4.1 Rossby Number

The relative importance of Coriolis forces to other inertial forces (e.g. centrifugal forces) depends on the flow velocity, the angular velocity of the reference frame, and a length scale describing the intended trajectory of the flow. The combination of these factors is described by the Rossby number (Ro) which is a ratio of the flow velocity (U) to a length scale (e.g. channel width) and the Coriolis parameter. In terms of submarine channels, different Rossby numbers may be calculated using either radius of channel curvature (R) (Equation 2.4.2) or channel width (W) (Equation 2.4.3) as a length scale (Wells and Cossu 2013).

$$Ro_r = {}^{U}/_{Rf} \qquad (2.4.2)$$

$$Ro_w = {}^{U}/_{Wf} \qquad (2.4.3)$$

These ratios describe the relative importance of Coriolis forces to other inertial forces, mainly centrifugal force. Flows with lower Rossby numbers are more influenced by Coriolis forces (i.e. $Ro_r < 1$, $Ro_w < 10$), whereas higher Rossby numbers describe conditions in which Coriolis forces are less important, and centrifugal forces dominate (i.e. $Ro_w > 10$, $Ro_r > 1$). In general terms, slower flows at higher latitudes with larger radii of trajectory are more influenced by Coriolis forces.

2.5 Channelized Turbidity Current Velocities

Velocity of turbidity flows is a key parameter in evaluating the influence of Coriolis forces. However, since modern turbidity flows are often infrequent and difficult to measure, there have been relatively few direct measurements of turbidity current velocities, particularly in the deep sea (e.g. Xu et al., 2004, Khirpounoff et al., 2003, Heezen and Ewing 1952). One of the earliest observations of turbidity flow velocity was by Heezen and Ewing (1952) who inferred the velocity of flows generated by the 1929 Grand Banks earthquake using the timing of communication cable breaks. More recently, measurements from moorings in the Zaire channel measured average velocities exceeding 1.21 m s^{-1} during a turbidity flow captured at 4000 m depth (Khripounoff et al., 2003). Measurements from the Monterey Channel by Xu et al., (2004) demonstrated the first in-situ observations of the vertical velocity profile of a turbidity current, with maximum velocities of 1.90 m s^{-1}. Turbidity current velocities have been considered to have an average velocity of 1 m s^{-1} when evaluating Ro of global datasets (Cossu et al., 2013).

Due to the lack of direct observation of channel forming turbidity currents, several methods have been developed to estimate turbidity flow parameters from resultant sediments and channel morphologies of modern channels (e.g. Komar 1969, Klaucke et al., 1997, Komar 1985). These methods are subdivided into two categories: 1) those that use sediment data from core samples (Komar 1985, Klaucke et al., 1997), and 2) those that rely on modern channel morphologies (e.g. Komar 1969, Klaucke et al 1997). Velocity estimates from these two strategies have been used to produce similar estimates in such study areas as the Amazon Channel in which a large volume of morphological and sedimentological data are available (e.g. Pirmez and Irman, 2003).

Komar (1969) identified relationships between modern channel morphology and flow parameters using a cross-channel momentum balance approach based on a uniform bankfull flow

(i.e. a turbidity flow that fills the channel between crests of bounding levees). In this relationship, Komar considers the Coriolis forces, centrifugal forces, and the pressure gradient forces caused by the supra-elevation of the flow to be in balance with each other. Under these assumptions, the upper slope of a channelized turbidity current (known as the "interface") is related to primary variables of flow velocity and flow density (Equation 2.5.1).

$$\frac{\Delta H}{W}\left[\frac{\rho_t - \rho}{\rho_t}\right] g = f(u) \pm \frac{(u)^2}{R} \qquad (2.5.1)$$

This approach assumes that the height of the right-hand and left-hand levees approximate the interface of a formative turbidity current at bankfull conditions. With this assumption, Komar (1969) uses morphological parameters (Figure 2.8) of the modern channel width (W), radius of channel curvature (R) and levee asymmetry (ΔH) to approximate the interface of the channel-forming turbidity current (Komar 1969). This equation also uses the Coriolis parameter, which is easily calculated with latitude (θ) and Earth's rotational velocity (Ω) in Equation 2.3.1. The two unknowns in Equation 2.3.4 are flow velocity (u) and flow density (ρ_t). The sign of the $\pm$ operator in Equation 2.3.4 depends on the direction of the channel curve. For example, in the northern hemisphere, Coriolis forces and centrifugal forces will reinforce each other in leftward bends of the channel axis and the operator will be positive. During right turns, these forces will oppose and the operator will be negative.

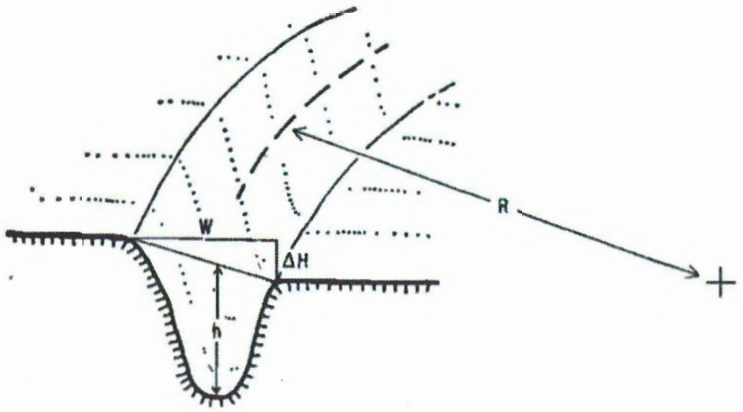

Figure 2.8 Spatial relationship between parameters of levee asymmetry (ΔH), radius (R), average channel depth/height (h) and channel width (W) used to calculate turbidity current velocity (from Komar 1969).

Velocity may be solved with Equation 2.5.1 by using assumptions of flow density, allowing calculation of the channel-forming turbidity current velocities using channel geometry. Applying this method the Monterey Fan channel, Komar (1969) predicted velocities between 6.0 – 20.0 m s^{-1}. This method was later applied to the Amazon Channel to estimate flow velocities between 0.5 – 3.5 m s^{-1} and was observed to produce similar estimates to sediment derived velocities (Pirmez and Imran 2003).

Further development of this technique by Bowen et al., (1984) incorporated the use of a densiometric Froude number (Fr^2) which could be estimated from the channel floor slope (β) (Equation 2.5.2).

$$Fr^2 = \frac{tan\beta}{(1+a)C_f} \qquad (2.5.2)$$

Assumptions of the frictional drag coefficient ($C_f = 0.004$) and an interface drag ratio (α) can be implemented to reduce uncertainties from the need to estimate flow density in this approach (Klaucke et al., 1997). The result is an equation for calculating velocity without making assumptions about flow density as approximated from grain size data (Equation 2.5.3).

$$u = \frac{2\Omega sin\phi}{\frac{\Delta H}{WHF_r{}^2} \pm \frac{1}{R}} \qquad (2.5.3)$$

This approach was applied to the NAMOC to estimate average velocities 0.86 m s^{-1} (Klaucke et al., 1997).

2.5 Global Trends in Channel Sinuosity

By re-examining and updating the compilation of global sinuosity data used by Clark et al. (1992) to establish slope/sediment relationships, Peakall et al (2012) discovered an apparent correlation between latitude and peak channel sinuosity. In this relationship, peak channel sinuosity was observed to be inversely correlated to latitude with an exponential best fit R^2 value of 0.63 (Figure 2.9).

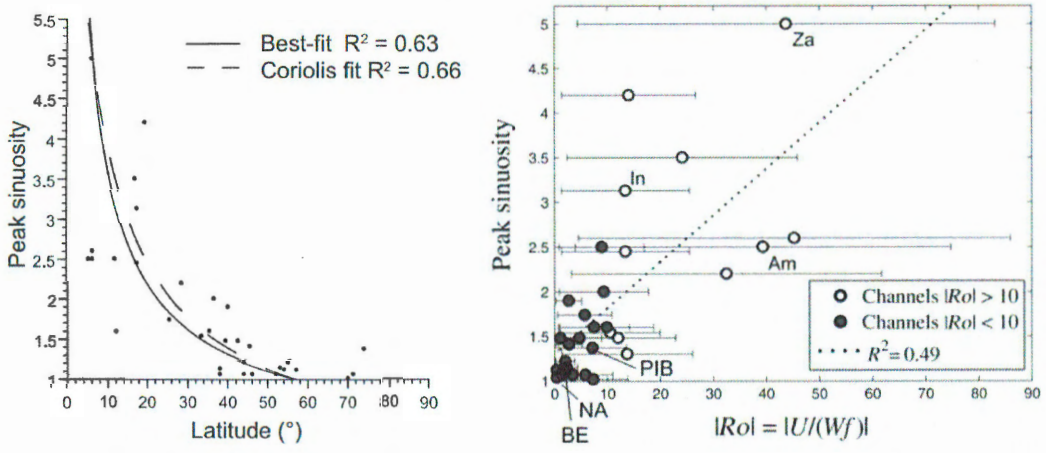

Figure 2.9 Left: Correlation between submarine channel peak sinuosity and latitude (from Peakall et al., 2012). Right: Associated Ro_w values calculated using a velocity of 1 m s^{-1}, showing the relationship between low sinuosity channels and low Rossby numbers (from Cossu et al., 2013).

While other factors such as sediment type, slope, climate and basement bathymetry are known to influence sinuosity (e.g. Clark et al 1992), Peakall et al. (2012) noted that the only factor to vary systematically and reliably with latitude was the strength of the Coriolis parameter. This observation led to a hypothesis that variations in strength of Coriolis forces with latitude play an important role in establishing the observed global variation in sinuosity (Peakall et al., 2012).

The suggestion of Coriolis force as a driving factor in this relationship was controversial, and promoted discussion in the literature. Sylvester et al., (2013) called into question the use of peak sinuosity as a comparative measure seeing as many channels may not reach maximum potential sinuosity of the system due to local slopes that are either too steep or too shallow for optimal sinuosity development. Sylvester et al., (2013) also suggested that Coriolis is likely to have little to no effect on the faster, higher-density flows that are known to influence channel path (citing Pirmez et al., 2003). In a reply, Peakall et al., (2013) reaffirm the use of peak sinuosity measure, which is noted to be the only measurable parameter to enable sinuosity comparisons between channel systems. This measure also reduces the influence of local factors influencing sinuosity within a single channel system that may alter sinuosity along the channel length. Peakall et al., (2013) note that there is appreciable error involved in peak sinuosity measurements resultant from the scale over which they are made (i.e. number of meanders, km

scale). They suggest that channels initiating along relatively straight paths at high latitudes will be substantially influenced by the Coriolis effect, and thus maintain a straighter planform geometry. Both authors agree that control on channel path development is a multifactorial process, and global datasets are likely to be influenced by several local drivers in addition to Coriolis forcing.

To examine the potential influence of Coriolis forces on channel-forming turbidity currents in greater detail, tabletop gravity current modelling studies using rotating gravity current platforms were undertaken to examine flow circulation and intra-channel deposition/erosion under various simulated Rossby conditions (Cossu et al., 2013, Wells and Cossu 2013, Cossu and Wells 2010). By changing the rate of rotation, these experiments effectively isolated the influence of different Rossby conditions (i.e. latitude analog) by keeping current flow parameters, trajectory and erodible sediment characteristics constant. These experimental approaches demonstrated that at low Rossby numbers; flows exhibit tilted interfaces, changes in secondary circulation patterns (Cossu and Wells 2010), decreases in velocity, and shifting of the velocity maximum within the flow (Cossu and Wells 2013).

The influence of Coriolis deflection on intrachannel deposition and erosion patterns was demonstrated by rotating erodible beds at high angular velocities to simulate low Rossby conditions (Figure 2.10). Wells and Cossu (2013) suggest that the shifting of the velocity maximum of the turbidity current may provide a mechanism by which sinuosity growth is inhibited in high latitude channels. In this model, the deflection of the velocity core of the flow to one side of the channel prevents meanders from amplifying, thus maintaining a straighter channel path and possibly influencing patterns of deposition and erosion within the channel (Figure 2.11).

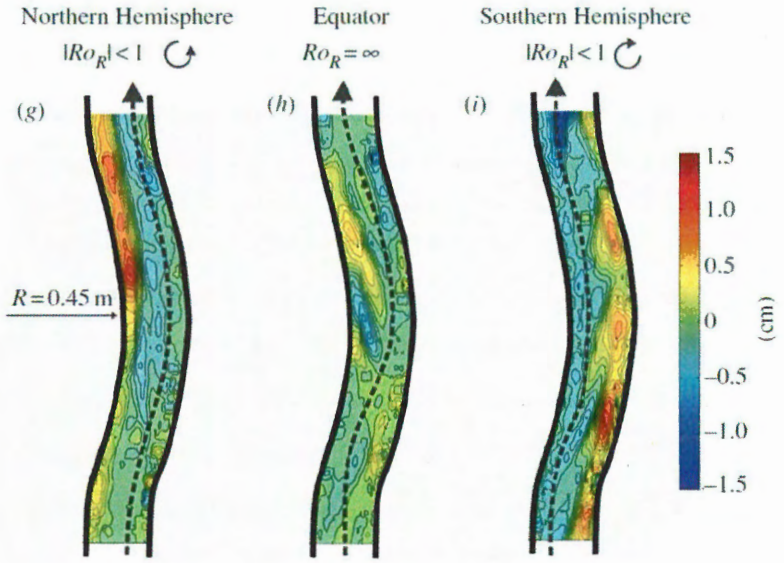

Figure 2.10 Select results modified from Wells and Cossu (2013) showing erosion/deposition maps (g-i) of rotating channels under different Rossby conditions representative of high latitude and equatorial conditions. Location of the velocity maximum is denoted by the dashed arrow.

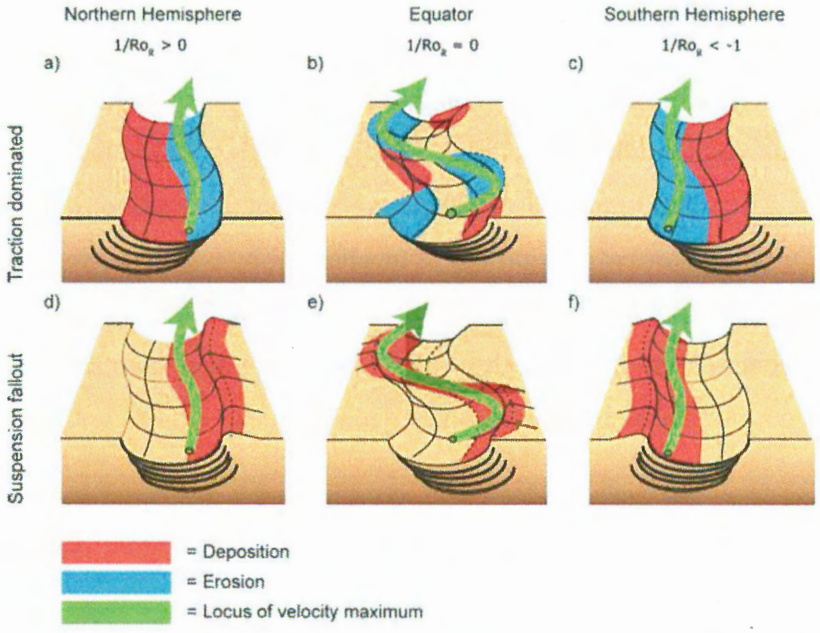

Figure 2.11 Illustrated model from Cossu et al., (2015) synthesizing the results of experimental low Rossby currents. Note that the deflection of the turbidity current velocity maximum influences deposition and erosion patterns for suspension dominated and traction dominated flows.

Synthesized by Cossu et al., (2015), this model is also expected to influence suspension dominated and traction dominated portions of gravity currents differently (Figure 2.11). In the northern hemisphere, suspension dominated flows will be deflected to the right such that deposition by suspension fall-out of these sediments will occur preferentially on the right-hand side of the channel. This phenomenon results in the construction of large external levee channel asymmetries in which the righthand levee is larger than the lefthand levee (e.g. NAMOC). This preferential levee building also promotes channel migration to the left-hand side.

Deposits by traction-dominated flows in the northern hemisphere would appear to have an opposite directional sense to the deposits of suspension dominated flows according to the model of Cossu et al., (2015). For these flows, deflection of the velocity maximum would promote erosion on the right-hand side and deposition on the left-hand side. This geometry would promote channel migration to the right where traction-dominated processes dominate.

2.6 Other high-latitude channel systems

One of the most prominent and well-studied high latitude submarine channel systems is the North Atlantic Mid Ocean Channel (NAMOC) that stretches >3000 km from the southern limit of Baffin Bay and Davis Strait, through the Labrador Sea and around Newfoundland, to the Sohm Abyssal Plain. This channel system is an example of a low-gradient, low-sinuosity abyssal channel and has served as a major sediment conduit in the North Atlantic.

The channel has prominent external levees with consistent right-hand levee asymmetry that is maintained over most of the channel length (Figure 2.12). This characteristic is interpreted to indicate that Coriolis forces are consistently dominant to centrifugal forces in terms of the integrated flow field and suspension-dominated flows (Klaucke et al., 1997, Cossu et al., 2015). The channel consists of three genetically different morphological domains related to different control mechanisms of the channel path. These include an upper equilibrium channel, middle modified equilibrium channel, and lower basement-controlled channel (Klaucke et al., 1997).

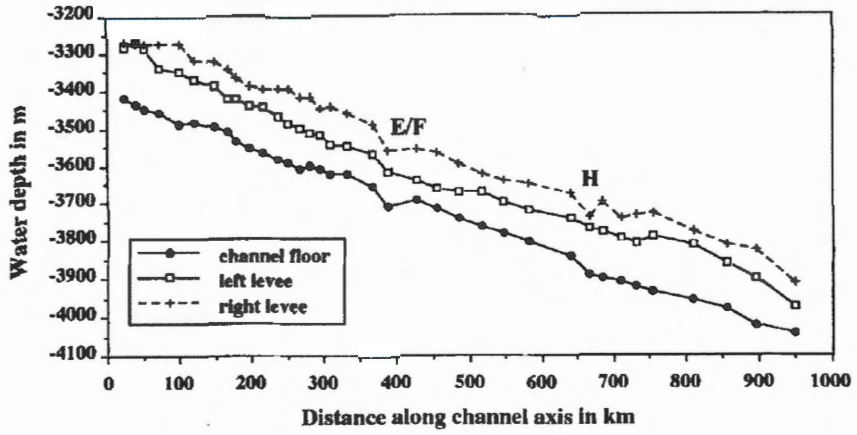

Figure 2.12 Water depths of the channel floor, left levee and right levee of the North Atlantic Mid Ocean Channel north of 53°N (from Klaucke et al., 1997).

Cossu et al., (2015) examined the intrachannel architecture of NAMOC in the context of Coriolis deflection of the velocity maximum. They note that intra-channel deposits of the lower sinuous reach of NAMOC do not consistently follow regular point bar accretion models of Coriolis-neutral channels, nor do they consistently follow the models of high latitude channels from Wells and Cossu (2013). Because of this, they suggest that the influence of Coriolis on these intrachannel deposits may not be consistent throughout the whole system (Cossu et al., 2015), despite the clear dominance of Coriolis forces on the asymmetric external levees.

Where the channel appears to be erosional/traction-dominated, intrachannel morphologies are largely similar to results of experimental models of low Rossby numbers by Wells and Cossu (2013). Internal terraces are also described to be narrow compared to the width of the channel (Cossu et al., 2015). This observation prompted the interpretation that these terraces are self-limiting, and may not accrete laterally to drive amplification of meander bends as do point bars in classic sinuosity models (Cossu et al., 2015).

Cossu et al., (2015) note the difficulties in distinguishing which features of the modern channel morphology are the result of suspension dominated vs. traction dominated flows in NAMOC. Here, the authors note that intrachannel geometry is complicated by the influence of channel wall sliding, inherited bathymetry, and intrinsic variations between suspension-dominated and traction-dominated flow regimes during channel development. In their analysis, they consider reaches without substantial channel incision to be characteristic of suspension-

dominated flows. Conversely they consider reaches with substantial incision and minimal levee formation to be characteristic of more traction-dominated regimes.

Other examples of high latitude channels include the Kongsfjorden Channel System (Forwick et al., 2015), Lofoten Basin Channel (Dowdeswell et al., 1996), the Inbis Channel (Vorren et al., 1998), as well as channel systems off Eastern Greenland (Wilken and Mienert 2006), the South Weddell Sea (Michels et al., 2002) and the North Antarctic Peninsula (Rebesco et al., 2002). Recent discoveries in the Arctic Ocean include the 160 km long "Weather Channel" draining from the Chukchi Rise into the Canada Basin (Mayer et al., *In press*). Hypotheses concerning the genesis of these channels are varied but generally include; transformation of glacial debris flows, hypercycnal flow at ice margins or riverine outputs, and oceanographic resuspension of shelf sediments (e.g. Piper and Normark, 2009).

3.0 Methods

Data collected in the past decade offer the opportunity to study the morphology of the NP-28 channel in enough detail to compare with experimental models of high latitude channels. This chapter details data sources, acquisition, processing, and analyses used in this project.

3.1 Data Acquisition

Ice Conditions

Data collection in the Amundsen Basin is made challenging due to perennially thick ice conditions. Sea-ice circulation in this region is driven by the interaction of the Beaufort Gyre and Transpolar Drift which direct sea-ice towards the shores of northern Greenland. In the Amundsen Basin, this results in the build-up of thick (up to 4 m) multiyear ice, significant ice ridging (up to 30 m) and conditions up to 10/10ths ice cover (Figure 3.1, Figure 3.2). Subbottom and multibeam data collected in these conditions are prone to high levels of noise from icebreaking operations and may experience gaps where signal is lost. Complete data coverage is often not possible due to the limitations placed on survey operations by these ice conditions.

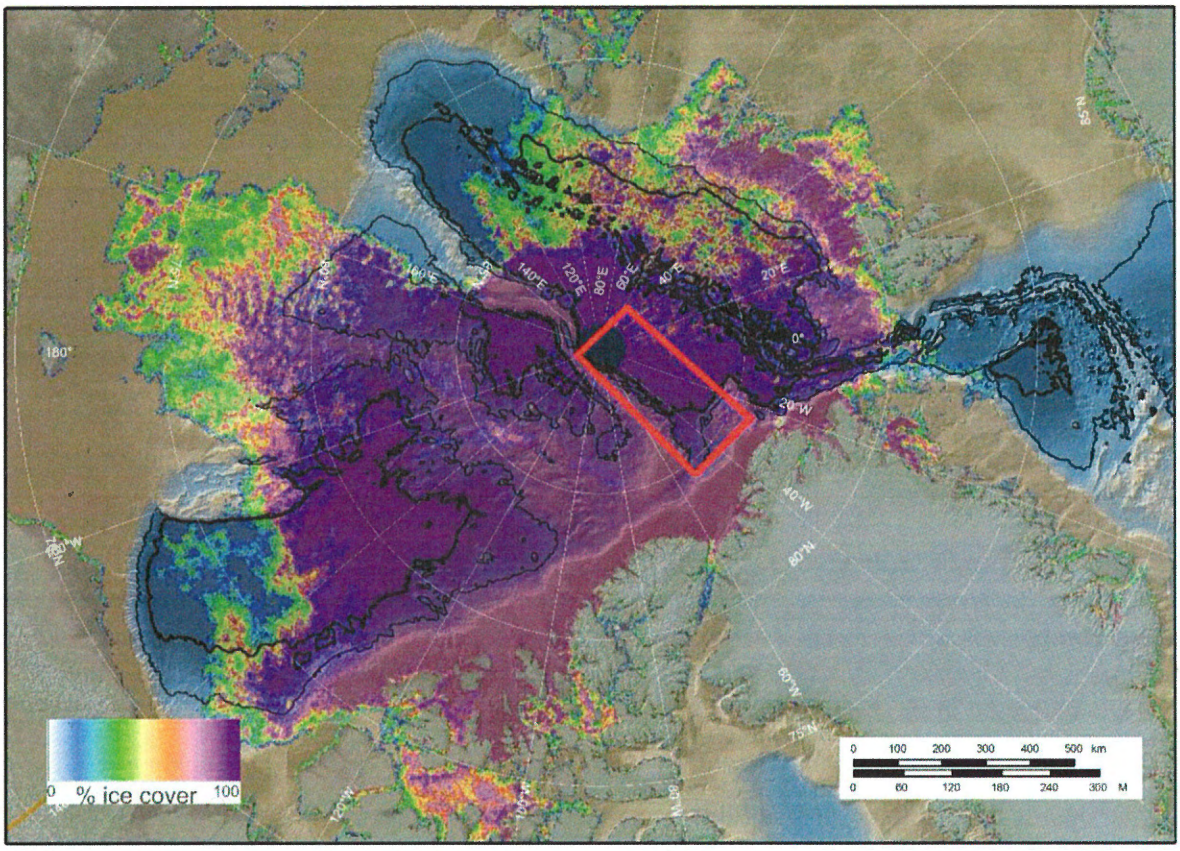

Figure 3.1 Advanced Microwave Scanning Radiometer – EOS (AMSR-E) image of sea ice minimum for the Arctic Ocean in 2014. Study area is outlined in red.

5.4.3 Overbank Element: Sediment Waves

Sediment waves are common features of submarine channel-levee systems (Normark et al., 2002, Normark et al., 1980, Wynn et al., 2000) and are thought to be the result of Froude supercritical flows of an unconfined turbidity current, bounded by hydraulic jumps (e.g. breaks in slope) in the levee surface (Fildani et al., 2006). The upslope-migration of these waves is the result of supercritical flow that provides conditions for antidunal development of waveforms. Similar examples of these structures have been imaged by high resolution seismic systems on the Monterey Fan (Normark et al., 2002) and Delgada Fan (Normark and Gutmacher, 1985) among others.

Previous attempts were made to relate these types of sediment waves to flow parameters of overbank flows (Normark et al., 1980, Flood, 1988, Wynn et al., 2000). A simple two-layer model used by Normark et al., (1980) relates the height of the overbank flow to a densiometric Froude number (Equation 5.1).

$$L_{sw} = \frac{2\pi(u^2)}{g_0 C} = 2\pi(Fi^2)h \qquad (5.1)$$

Assumptions of a Froude number of 1 (due to the interpretations of supercritical conditions necessary for the deposition of antidunal structures), Normark et al., (1980) simplify Equation 5.1 to an expression in which wavelength of the sediment waves (L_{sw}) is roughly one-sixth the height of the responsible flow (h) (Equation 5.2).

$$h = \frac{L_{sw}}{2\pi} \qquad (5.2)$$

Adopting these assumptions, measurements of average wavelengths from the NP-28 levee backslopes imply overbank flow heights of 32 to 85 m. As noted by Wynn et al., (2000) the applicability of the antidune model to these deepwater settings has substantial uncertainty, and is made with caution.

5.4.4 Channel Element: Distributary Channel

Distributary channels are a common feature of many fan systems, and may be generated by different processes. In the case of several fan-related channel systems, such as the Amazon Channel, distributaries are most commonly formed by channel avulsion events and are generally

related to channel wall failures or levee breaches along channel meanders (Wynn et al., 2007). These events establish a new channel baselevel, create a knickpoint in the longitudinal channel profile (Pirmez et al., 1995) and result in abandonment of the old channel (Wynn et al., 2007).

The longitudinal profile of the NP-28 main channel appears to show a slight increase in gradient at ~350 km down-channel distance, similar to knickpoints observed in the Rhône channel system where the longitudinal profile has not yet reached equilibrium following channel avulsion (Bonnel et al., 2005). However, the distinct difference in channel widths between the NP-28 distributary channel and the main channel would suggest they are the result of different processes, and thus might not be explained by avulsion of a single channel form. Furthermore, the perceived knickpoint is very slight, and of a much smaller magnitude than knickpoints observed in other systems where avulsion has occurred (e.g. Rhône Fan channel). This perceived increase in gradient is likely better explained by the local incision of the thalweg by confined flows.

It is suggested that the distributary observed in the lower fan was formed as a result of erosion by flow-stripped currents from the main channel. This result is supported by observations of the supra-elevation of the distributary thalweg compared to the main channel thalweg, shoaling of the seafloor between the distributary channel and Lomonosov Ridge, and channel floor reflections that strongly resemble distributary levee characteristics in subbottom profiler data. Decreases in distributary channel height towards the branching point may be a result of the initial erosion by the flow-stripped currents during its development, or progressive infilling by overbanking sediments from the main channel axis.

The initial erosion of this channel may also have been related to the ~1.6 km wide knoll feature observed in multibeam bathymetry. This feature could have influenced overbanking flows, and resulted in localized erosion and channel formation of the downslope surface.

Since there is no data coverage over the assumed branching point with the main channel, it is difficult to assess whether this flow stripping hypothesis is supported by a low point in the left-hand levee. Further data collection may be able to better constrain the processes responsible for the genesis of this distributary channel.

5.5 Velocity Estimation

Bankfull velocities for the lower channel were estimated to an average of 0.38 m s^{-1} using morphological parameters of the channel extracted from multibeam coverage in Equation 2.5.3. This estimate falls within ranges expected for bankfull flow estimates for submarine channels (Konsoer et al., 2013) but is substantially lower than morphometrically determined flow velocities of NAMOC turbidity currents, which were estimated to be an average of 0.86 m s^{-1} (Klaucke et al., 1997).

Cossu et al., (2010) experimentally demonstrated that gravity flows under low Rossby conditions exhibited reduced downstream velocity compared to high Rossby flows with the same density contrasts. This suggests that identical flows at higher latitudes would be characteristically slower than lower latitude flows. However, downslope flow velocities of actual turbidity currents are likely much more influenced by sediment load, flow initiation processes (Piper and Normark, 2009) and slope than Coriolis forces, and thus differences between systems are more likely to reflect these factors. In the case of the NP-28 channel, further work and sampling may be able to further constrain the estimates of flow velocities using sediment derived techniques.

5.6 Coriolis and Sinuosity

Sinuosity results from the revised channel map indicate that the NP-28 channel is a low-gradient, low-sinuosity channel rather than a highly-sinuous channel as suggested by interpretations of Kristoffersen et al., (2004). This fits in the context of global sinuosity trends identified by Peakall et al., (2012) who demonstrated that peak sinuosity is inversely related to latitude. However, due to the potential for structural control on channel path and ambiguities in the understanding of sediment characteristics in this fan, it is difficult to use peak sinuosity alone to support or revise hypotheses concerning Coriolis forces and their influence on channel path development.

Instead, deposit geometry is better used to examine the influence of Coriolis on the NP-28 channel. The observations of consistent right-dominated external levee asymmetry prompts the interpretation that Coriolis forces dominated centrifugal forces for bankfull, suspension-dominated flows. These observations are consistent with low Rossby numbers calculated using

morphologically obtained velocities, and assumed velocities of 1 m s^{-1}. These mirror observations and interpretations of NAMOC, which exhibits the same characteristic right-dominant levee asymmetry (Cossu et al., 2015, Klaucke et al., 1997).

Geometries of internal levees and the modern thalweg of the channel in the lower fan are comparable to experimental results from rotating erodible bed studies obtained by Wells and Cossu (2013). In these studies, the thalweg and velocity maximum are deflected to the right side of the channel at simulated northern latitude conditions. The similarity between these geometries in the lower channel suggests linkages between the mechanisms described by Wells and Cossu (2013) and the observed intrachannel architecture in the NP-28 channel. This mechanism appears to be noticeably absent in the mid-fan region where outer bank erosion is observed. These observations indicate that the influence of Coriolis on traction dominated flows is not consistent over the entire channel, similar to what Cossu et al., (2015) described for the NAMOC.

6.0 Conclusions

The NP-28 channel is a low-gradient, low sinuosity channel that acted as a sediment pathway for turbidity currents flowing from the Klenova Valley of the Lincoln Sea into the Amundsen Basin of the greater Arctic Ocean. The channel runs >450 km parallel to Lomonosov Ridge and consists of a large main channel with a smaller distributary channel, interpreted to be the result of erosion by flow stripped currents. The modern morphology of this channel is a result of the action of large mixed turbidity currents, which have been substantially influenced by Coriolis forces

Peak sinuosity of the channel conforms to recently identified trends in channel sinuosity with latitude, however structural influence on channel path imposed by Lomonosov Ridge makes it difficult to assess its relevance. Despite this, partial similarities in the intrachannel architecture to tabletop studies examining deposition and erosion at low Rossby numbers suggest possible linkages in mechanisms that maintain straighter channel paths at high latitudes.

Modern geometry of the NP-28 channel shows evidence of a mixture of suspension and traction-dominated flow regimes. Aggradation of large asymmetrical levees is likely to have resulted from suspension-dominated flows. Estimates of average bankfull flow velocities using channel morphology suggest flows of 0.38 m s^{-1} and corresponding Rossby number calculations

indicate a strong influence of Coriolis forces on these flows. Coriolis deflections caused preferential deposition of overbank sediments on the right-hand levee of the channel, promoting substantial westward migration of the channel axis. These overbanking flows became supercritical on the backslopes of these levees, resulting in the formation of low-amplitude sediment wave fields.

The deposition of internal levees and thalweg incision within the NP-28 channel are explained by the influence of late-stage underfit traction-dominated flows. A slight knickpoint in the longitudinal gradient of the main channel axis is likely a result of incision along the lower channel segment by these traction dominated flows.

Comparison of intrachannel deposits to experimental models of high latitude channels indicates that the relative influence of Coriolis forces on intrachannel geometry is observed to vary along channel length. Near the mid-fan, outer bank erosion indicates that traction-dominated flows were likely to be faster than 1.49 m s^{-1} and Coriolis forces were likely to have little influence on the position of the velocity maximum. Deceleration of these flows, straighter bounding channel paths, and increases in strength of the Coriolis parameter with down-channel distance result in deposits that appear to be more influenced by Coriolis forces towards the distal culmination of the channel. In this part of the channel, the geometry of internal confined levees matches closely with experimental results for flows with low Rossby numbers, and suggests possible linkages between these deposits and recently proposed mechanisms for the maintenance of low sinuosity channel paths.

References

Babonneau N, Savoye B, Cremer M, Bez M. 2004. Multiple terraces within the deep incised Zaire Valley (ZaïAngo Project): are they confined levees? In: Confined Turbidite Systems. *Editors:* Lomas SA, Joseph P. Geological Society, London, Special Publications. 222. 91-114.

Backman J, Jakobsson M, Løvlie R, Polyak L, Febo LA. 2004. Is the central Arctic Ocean a sediment starved basin? *Quaternary Science Reviews*. 23: 1435-1454.

Bonnel C, Dennielou B, Droz L, Mulder T, Berné S. 2005. Architecture and depositional pattern of the Rhône Neofan and gravity activity in the Gulf of Lions (western Mediterranean). *Marine and Petroleum Geology*. 22: 825-843.

Bowen AJ, Normark WR, Piper DJ. 1984. Modelling of turbidity currents on Navy Submarine Fan, California Continental Borderland. *Sedimentology*. 31: 169-185.

Carter L, Carter RM. 1988. Late Quaternary development of left-bank-dominant levees in the Bounty Trough, New Zealand. *Marine Geology*. 78(3-4): 185-197.

Clark JD, Kenyon NH, Pickering KT. 1992. Quantitative analysis of the geometry of submarine channels: Implications for the classification of submarine fans. *Geology*. 20: 633-636.

Clark JD, Pickering KT. 1996. Submarine Channels: Processes and Architecture. *Vallis Press, London. 231 p.*

Courtney R. 2009. SegyJP2 Help Files. Natural Resources Canada, Bedford Institute of Oceanography, Dartmouth, NS. Available from: ftp://ftp.nrcan.gc.ca/gsc/courtney/SegyJp2/SegyJp2.htm

Cossu R, Wells MG. 2010. Coriolis forces influence the secondary circulation of gravity currents flowing in large-scale sinuous submarine channels systems. *Geophysical Research Letters*. 37: L17603.

Cossu R, Wells MG, Wåhlin AK. 2010. Influence of the Coriolis force on the velocity structure of gravity currents in straight submarine channel systems. *Journal of Geophysical Research*. 115: C11016.

Cossu R, Wells MG. 2013. The possible role of Coriolis forces in structuring large-scale sinuous patterns of submarine channel-levee systems. *Phil Trans R Soc A*. 371.

Cossu R, Wells MG, Peakall J. 2015. Latitudinal variations in submarine channel sedimentation patterns: The role of Coriolis forces. Journal of the Geological Society. 172(2): 161-174.

Covault JA, Fildani A, Romans BW, McHargue T. 2011. The natural range of submarine canyon-and-channel longitudinal profiles. *Geosphere*. 7(2): 313-332.

Deptuck ME, Steffens GS, Barton M, Pirmez C. 2003. Architecture and evolution of upper fan channel-belts on the Niger Delta slope and in the Arabian Sea. *Marine and Petroleum Geology*. 20: 649-676.

Døssing A, Hansen TM, Olesen AV, Hopper JR, Funck T. 2014. Gravity inversion predicts the nature of the Amundsen Basin and its continental borderlands near Greenland. *Earth and Planetary Science Letters*. 408: 132-145. doi: 10.1016/j.epsl.2014.10.011

Dowdeswell JA, Kenyon NH, Elverhøi A, Laberg JS, Hollender FJ, Mienert J, Sieger MJ. 1996. Large-scale sedimentation on the glacier-influence Polar North Atlantic margins: long-range side-scan sonar evidence. *Geophysical Research Letters*. 23:3535–3538

Faugères JC, Stow DAV, Imbert P, Viana A. 1999. Seismic features diagnostic of contourite drifts. *Marine Geology*. 162: 1-38.

Fildani A, Normark WR, Kostic S, Parker G. 2006. Channel formation by flow stripping: large

scale scour features along the Monterey East Channel and their relation to sediment waves. *Sedimentology*. 53: 1265-1287.

Forwick M, Laberg JS, Hass HC, Osti G. 2015. The Kongsfjorden Channel System offshore NW Svalbard: downslope sedimentary processes in a contour-current dominated setting. *Arktos*. 1(1): 1-16.

GEBCO. 2003. Sixteenth meeting of the GEBCO Sub-Committee on Undersea Feature Names (SCUFN). *International Hydrographic Bureau, Monaco, 10-12 April 2003.*

Heezen BC, Ewing M. 1952. Turbidity currents and submarine slumps, and the 1929 Grand Banks Earthquake. *American Journal of Science*. 250: 849-878.

Jackson HR, Dahl-Jensen T, Chian D, Shimeld J, Funck T, Asudeh I, Snyder D. 2010. Sedimentary and crustal structure from the Ellesmere Island and Greenland continental shelves onto the Lomonosov Ridge, Arctic Ocean. Geophys. J. Int. 182: 11-35

Jokat W, Weigelt E, Kristoffersen Y, Rasmussen T, Schöne T. 1995. New insights into the evolution of the Lomonosov Ridge and the Eurasian Basin. *Geophysical Journal International*. 122: 378-392.

Jokat W, Uenzelmann-Neben G, Kristoffersen Y, Rasmussen TM. 1992. Lomonosov Ridge – a double sided continental margin. *Geology*. 20: 887-890.

Jokat W, Micksch U. 2004. Sedimentary structure of the Nansen and Amundsen basins, Arctic Ocean. Geophysical Research Letters. 31 (L02603): 1-4.

Jakobsson M, Mayer L, Coakley B, Dowdeswell JA, Forbes S, Fridman B, Hodnesdal H, Noormets R, Pedersen R, Rebesco M, et al. 2012. The International Bathymetric Chart of the Arctic Ocean (IBCAO) Version 3.0. *Geophysical Research Letters*. 39(12).

Khripounoff A, Vangriesheim A, Babonneau N, Crassous P, Dennielou B, Savoye B. 2003. Direct observation of intense turbidity current activity in the Zaire submarine valley at 4000 m water depth. *Marine Geology*. 194: 151-158.

Klaucke I, Hesse R. 1996. Fluvial features in the deep-sea: new insights from the glacigenic submarine drainage system of the Northwest Atlantic Mid-Ocean Channel in the Labrador Sea. *Sedimentary Geology*. 106: 223-234.

Klaucke I, Hesse R, Ryan WBF. 1997. Flow parameters of turbidity currents in a low-sinuosity giant deep-sea channel. *Sedimentology*. 44: 1093-1102.

Klaucke I, Hesse R, Ryan WBF. 1998. Seismic stratigraphy of the Northwest Atlantic Mid Ocean Channel: growth pattern of a mid-ocean channel-levee complex. *Marine and Petroleum Geology*. 15: 575-585.

Komar PD. 1969. The channelized flow of turbidity currents with application to Monterey Deep-Sea Fan Channel. Journal of Geophysical Research. 74(18): 4544-4558.

Komar PD. 1985. The hydraulic interpretation of turbidites from their grain sizes and sedimentary structures. *Sedimentology*. 32: 395-407.

Konsoer K, Zinger J, Parker G. 2013. Bankfull hydraulic geometry of submarine channels created by turbidity currents: Relations between bankfull channel characteristics and formative flow discharge. *Journal of Geophysical Research: Earth Surface.* 118: 216-228.

Kristoffersen Y, Sorokin MY, Jokat W, Svendsen O. 2004. A submarine fan in the Amundsen Basin, Arctic Ocean. *Marine Geology*. 204: 317-324.

Kristoffersen, Y. 2015. FRAM 2014/2015 Weekly Blogs: Weekly Report 27 [Website]. Retrieved March 18th, 2016 from: https://sabvabaa.nersc.no/node/329

Laberg JS, and Vorren TO. 2000. Flow behaviour of submarine glacigenic debris flows on Bear

Island Trough Mouth Fan, western Barents Sea. *Sedimentology.* 47: 1105-1117.
Mayer LA, Gardner JV, Armstrong AA. In press. An ultrahigh latitude submarine channel: northern Chukchi rise. *In:* Atlas of Submarine Glacial Landforms: Modern Quaternary and Ancient.
Menard, HW. 1955. Deep-sea channels, topography and sedimentation. American Association of Petroleum Geologists Bulletin. 39(2): 236-255.
Michels KH, Kuhn G, Hillenbrand CD, Diekmann B, Futterer DK, Grobe H, Uenzelmann-Neben G. 2002. The southern Weddell Sea: combined contourite-turbidite sedimentation at the southeastern margin of the Weddell Gyre. *Geological Society of London Memoirs*. 22: 305-323.
Moore, T.C., and the Expedition 302 Scientists. 2006. Sedimentation and subsidence history of the Lomonosov Ridge. In Backman, J., Moran, K., McInroy, D.B., Mayer, L.A., and the Expedition 302 Scientists. Proc. IODP, 302: Edinburgh (Integrated Ocean Drilling Program Management International, Inc.). doi:10.2204/iodp.proc.302.105.2006
Mutti E, Normark WR. 1991. An integrated approach to the study of turbidite systems. In: Seismic Facies and Sedimentary Processes of Submarine Fans and Turbidite Systems. Editors: Weimer P, Link MH. Springer Press, New York, NY: 75-106.
Normark WR, Hess GR, Stow DAV, Bowen AJ. 1980. Sediment waves on the Monterey Fan levee: A preliminary physical interpretation. *Marine Geology*. 37(1-2): 1-18.
Normark WR, Gutmacher CE. 1985. Delgada Fan, Pacific Ocean. In: Submarine Fans and Related Turbidite Systems. Editors: Bouma AH, Normark WR, Barnes NE. Springer-Verlag, New York, NY. 59-64.
Normark WR, Piper DJW. 1991. Initiation processes and flow evolution of turbidity currents: Implications for the depositional record. *In*: *From Shoreline to Abyss, Society of Economic Paleontologists and Mineralogists Special Publication*. 46: 207-230.
Normark WR, Piper DJW, Posamentier H, Pirmez C, Migeon S. 2002. Variability in form and growth of sediment waves on turbidite channel levees. *Marine Geology*. 192: 23-58.
Peakall J, McCaffrey B, Kneller B. 2000. A process model for the evolution, morphology, and architecture of sinuous submarine channels. *Journal of Sedimentary Research*. 70(3):434-448.
Peakall J, Amos KJ, Keevil GM, Bradbury PW, Gupta S. 2007. Flow processes and sedimentation in submarine channel bends. *Marine and Petroleum Geology*. 24: 470-486.
Peakall J, Kane IA, Masson DG, Keevil G, McCaffrey W, Corney R. 2012. Global (latitudinal) variation in submarine channel sinuosity. *Geology*. 40, 11-14.
Peakall J, Kane IA, Masson DG, Keevil G, McCaffrey W, Corney R. 2013. Global (latitudinal) variation in submarine channel sinuosity: REPLY. Geology. 41(5), e288.
Piper DJW, Hiscott RN, Normark WR. 1999. Outcrop-scale acoustic facies analysis and latest Quaternary development of Hueneme and Dume submarine fans, offshore California. *Sedimentology*. 46: 47-78.
Piper DJW, Normark WR. 2001. Sandy fans – from Amazon to Hueneme and beyond. *AAPG Bulletin*. 85(8): 1407-1438.
Piper DJW, Normark WR. 2009. Processes that initiate turbidity currents and their influence on turbidites: a marine geology perspective. *Journal of Sedimentary Research*. 79: 347-362.
Pirmez C, Beaubouef RT, Friedmann SJ, Mohrig DC. 2000. Equilibrium profile and baselevel in submarine channels: Examples from late Pleistocene systems and implications for the architecture of deepwater reservoirs. *In:* GCSSEPM Foundation 20th Annual Research

Conference: Deep-Water Reservoirs of the World. *Editors*: Weimer P, Slatt RM, Coleman J, Rosen NC, Nelson H, Bouma H, Styzen MJ, Lawrence DT. 782-805.

Pirmez C and Imran J. 2003. Reconstruction of turbidity currents in Amazon Channel. *Marine and Petroleum Geology*. 20: 823-849.

Pirmez C and Flood RD. 1995. Morphology and structure of Amazon Channel. *In:* Proceedings of the Ocean Drilling Program, Initial Reports. *Editors*: Flood RD, Piper DJW, Klaus A, et al. 155: 23-45.

Rebesco M, Pudsey C, Canals M, Camerlenghi A, Barker P, Estrada F, Giorgetti A. 2002. Sediment drift and deep-sea channel systems, Antarctic Peninsula Pacific Margin. *In:* Deep-Water Contourite Systems: Modern Drifts and Ancient Series, Seismic and Sedimentary Characteristics. *Editors:* Stow DAV, Pudsey CJ, Howe JA, Faugères JC, Viana AR. *Geological Society, London, Memoirs*. 22: 353-371

Rebesco M, Hernández-Molina FJ, Van Rooij D, Wåhlin A. 2014. Contourites and associated sediments controlled by deep-water circulation processes: State-of-the-art and future considerations. *Marine Geology*. 352: 111-154.

Schauer U, Rudels B, Jones EP, Anderson LG, Muench RD, Björk G, Swift JH, Ivanov V, Larsson AM. 2002. Confluence and redistribution of Atlantic water in the Nansen, Amundsen and Makarov basins. *Annales Geophysicae*. 20: 257-73.

Sylvester Z, Pirmez C, Cantelli A. 2011. A model of submarine channel-levee evolution based on channel trajectories: Implications for stratigraphic architecture. *Marine and Petroleum Geology*. 28: 716-727.

Sylvester Z, Pirmez C, Cantelli A, Jobe ZR. 2013. Global (latitudinal) variation in submarine channel sinuosity : Comment : Geology, e287.

Stein R. 2008. Chapter Three: Glacio-marine sedimentary processes. *In:* Arctic Ocean Sediments: Processes, Proxies, and Paleoenvironment. *Editors:* Stein R. Elsevier, Amsterdam. pp 87-126.

Svindland KT, Vorren TO. 2002. Late Cenozoic sedimentary environments in the Amundsen Basin, Arctic Ocean. *Marine Geology*. 186: 541-555.

Vorren TO, Laberg JS, Blaume F, Dowdeswell JA, Kenyon NH, Mienert J, Rumohr J, Werner F. 1998. The Norwegian–Greenland sea continental margins: morphology and late Quaternary sedimentary processes and environment. *Quaternary Science Reviews*. 7:273–302

Wells M, Cossu R. 2013. The possible role of Coriolis forces in structuring large-scale sinuous patterns of submarine channel-levee systems. *Phil Trans R Soc A*. 371: 20120366.

Wilken M, Mienert J. 2006. Submarine glacigenic debris flows, deep-sea channels and past ice-stream behaviour of the East Greenland continental margin. *Quaternary Science Reviews*. 25:784–810

Wynn RB, Cronin BT, Peakall J. 2007. Sinuous deep-water channels; genesis, geometry and architecture. *Marine and Petroleum Geology*. 24: 341-387.

Wynn RB, Masson DG, Stow DAV, Weaver PPE. 2000. Turbidity current sediment waves on the submarine slopes of the western Canary Islands. *Marine Geology*. 163: 185-198.

Xu JP, Noble MA, Rosenfeld LK. 2004. In-situ measurements of velocity structure within turbidity currents. *Geophysical Research Letters*. 31: L09311.

Appendices

I. Results of flow accumulation/least cost path

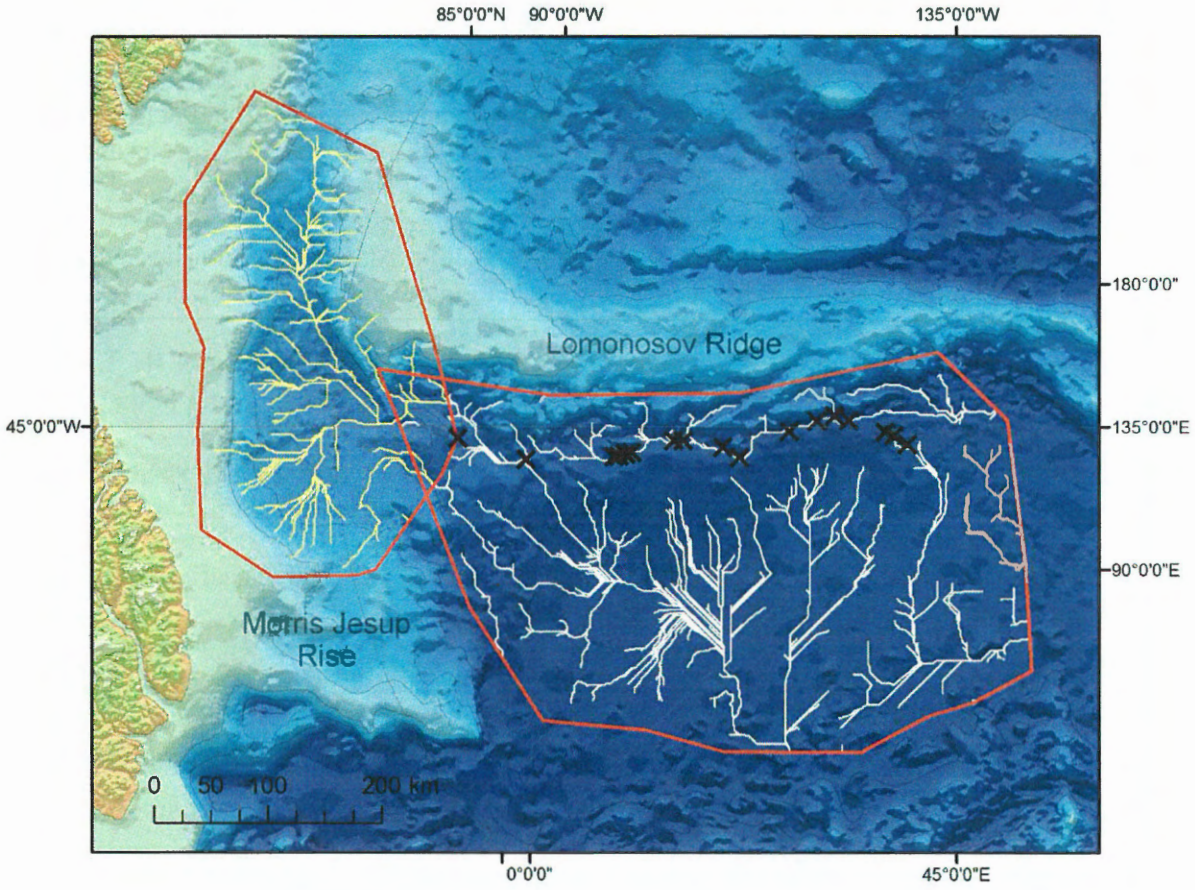

Figure A.1 Results of two flow accumulation analyses conducted using the IBCAO V3.0 grid. Red polygons indicated the clipped area used for each analysis. White and yellow stream networks indicate cells with greater than 750 grid cell accumulation. Black crosses indicate known locations of the channel from the data used in this project.

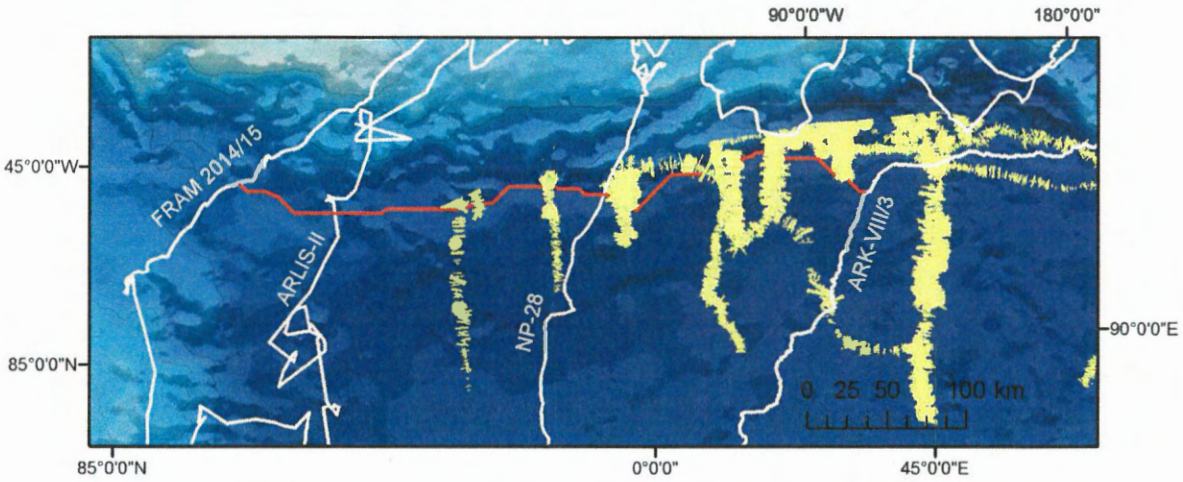

Figure A.2. Results of least cost path analyses (red) between tie points of known channel locations. Also shown is the coverage of multibeam data used in this study (yellow) and the tracklines of the FRAM 2014/15, NP-28 and ARLIS-II ice camps, and R/V Polarstern ARK-VIII/3 research expedition from which published seismic data have been acquired.

II. Previously published seismic sections used in this analysis

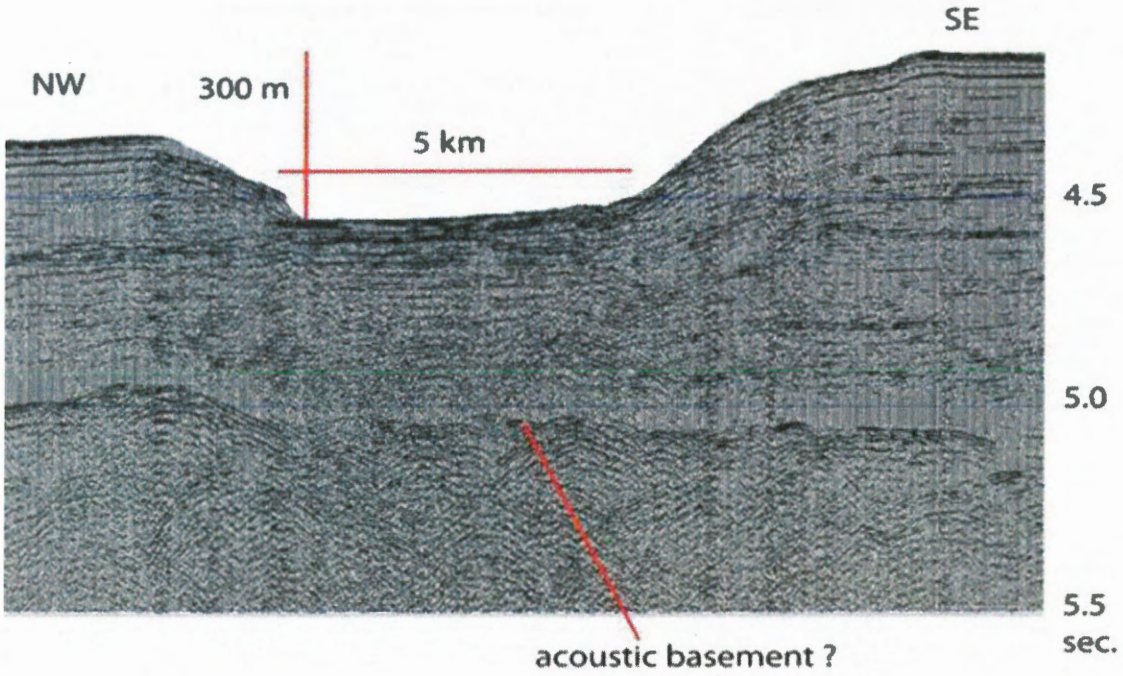

Figure A.3 Single channel sparker seismic section acquired by Kristoffersen et al., (2015) aboard R/H Sabvabaa during the FRAM 2014/2015 expedition.

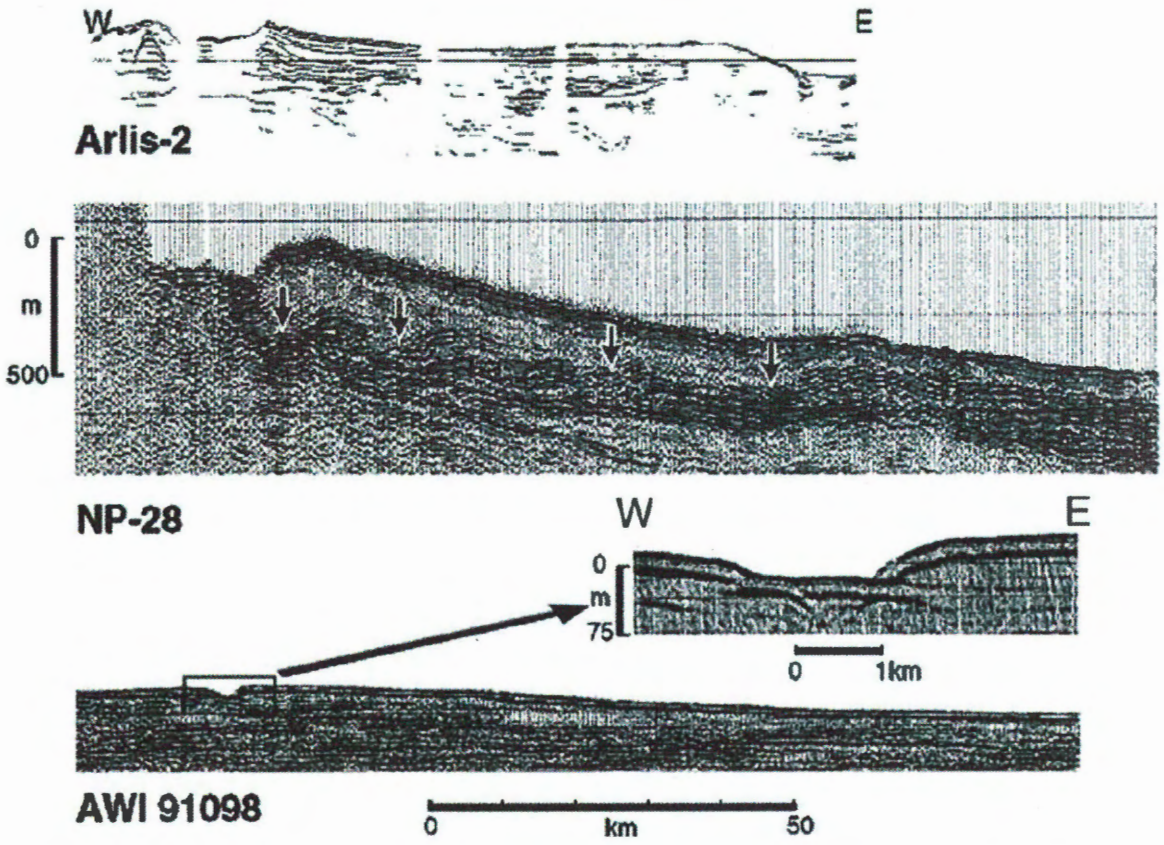

Figure A.4 Seismic sections from Kristoffersen et al., (2004) acquired by R/V Polarstern (AWI 91098, ARK-XIII/3), ARLIS-II and NP-28 ice camps.

DALHOUSIE UNIVERSITY
Inspiring Minds

Department of Earth Sciences
Halifax, Nova Scotia
Canada B3H 4J1
(902) 494-2358
FAX (902) 494-6889

DATE: April 29 2016

AUTHOR: Kai Boggild

TITLE: Morphological examination of the NP-28 submarine channel-fan complex in the Amundsen Basin, Arctic Ocean

Degree: BSc Convocation: _____ Year: 2016